ICCUB-14-043

Gauge/gravity dualities and bulk phase transitions.

Anton F. Faedo,[1] Maurizio Piai,[2] and Daniel Schofield[2]

[1]*Departament de Física Fonamental & Institut de Ciències del Cosmos, Universitat de Barcelona, Martí i Franquès 1, E-08028 Barcelona, Spain.*

[2]*Department of Physics, College of Science, Swansea University, Singleton Park, Swansea, Wales, UK.*

(Dated: April 28, 2014)

We consider D7-branes probing several classes of Type IIB supergravity backgrounds, and study the classical problem of finding equilibrium configurations for the embedding functions. This is a method employed to model chiral symmetry breaking in the gravity dual of a strongly-coupled, confining gauge theory. We unveil and discuss a new type of phase transition appearing in the gravity systems, which is similar in nature and meaning to bulk phase transitions on the lattice. The existence of this genre of phase transition puts a new, intrinsic limit on the region of parameter space which can be used to study the physics of the dual field theory. We complete the analysis of D7 embeddings in wrapped-D5 supergravity backgrounds, and explain in what cases chiral-symmetry breaking is sensibly modelled by the gravity construction.

arXiv:1402.4141v2 [hep-th] 25 Apr 2014

Contents

I. Introduction 1

II. Discussion. 2

III. The wrapped-D5 system. 5
A. Flavored Abelian solutions. 5

IV. D7 embedding. 6
A. Flavored Abelian backgrounds. 6

V. Chiral symmetry breaking in the wrapped-D5 system. 8
A. Non-Abelian solutions and the baryonic branch. 9
B. Walking solutions on the baryonic branch. 10
C. Summary. 12

VI. Conclusions and further directions. 13

Acknowledgments 14

References 14

I. INTRODUCTION

The study of strongly-coupled field theories is notoriously difficult. Traditional perturbation theory fails to capture non-perturbative phenomena, that become dominant at strong coupling. In the case of (four-dimensional) gauge theories there are two examples in which strong dynamics needs to be address: the study of QCD and of technicolor [1–3], a proposal for the origin of electroweak symmetry breaking (EWSB). In both cases, the strong dynamics induces the spontaneous breaking of (approximate) chiral symmetry.

A powerful tool in the study of realistic gauge theories in the strong-coupling regime is lattice field theory: one replaces the continuum space-time with a discretized space, which is amenable to numerical studies. Besides its practical utility, the lattice provides a sensible definition of the measure in the path integral.

String theory on curved backgrounds offers an alternative way of studying four-dimensional, strongly-coupled, field theories [4, 5]. This framework goes under the generic name of *gauge/gravity dualities*, and has the peculiarity that when the field theory is at strong coupling, its gravity dual (under suitable conditions) is weakly coupled. For example, this approach allows one to compute the Wilson loop of a gauge theory [6], to characterise confinement [7] and to discuss the properties of matter fields in a gauge theory [8].

Gauge/gravity dualities are based on a conjecture. Aside from strong evidence collected by systematically comparing physical quantities, certain formal procedures that are necessary in field-theory calculations can be seen to emerge also in the treatment of their gravity duals. The obvious example is holographic renormalisation [9]: when extracting physical (field-theory) results for correlation functions from the gravity theory, one has to implement a procedure closely reminiscent of renormalisation in field theory.

In this paper we show an example of a formal problem, emerging in certain gravity calculations, that has an analog in lattice gauge theory, and that forces us to implement a procedure similar to what is done on the lattice. On the one hand this provides another, new element to support the basic ideas of gauge/gravity dualities. On the other hand it has unexpected and important physical consequences, placing intrinsic limits on the regime of applicability of the dualities.

In the lattice literature, the analog of the phenomenon we want to discuss is that of *bulk* phase transitions. Generically, a lattice theory is different from the continuum field theory it intends to model. The finite lattice spacing introduces a new scale that can be thought of as some UV-regulator for the field theory. Furthermore, the operators (and symmetries) of the lattice are different from those of the continuum theory. However, provided the long-distance physics of the lattice and field theories

are in the same universality class, the lattice calculation yields useful results that also hold true in the continuum. The field theory is defined in terms of an RG fixed point of the lattice theory.

But it may occur that the lattice theory has a non-trivial phase structure, with lines (or hypersurfaces) of phase transitions (or crossovers) partitioning the parameter space. Thus, one has to make sure that the region of parameter space that the calculation is probing is restricted to the patch that is connected to the relevant fixed point, and hence belongs to the same universality class as the field theory. In general, this imposes bounds on the magnitude of the parameters in the lattice action.

An example of this phenomenon is the bulk phase-transition that appears in $SU(N)$ Yang–Mills theories as a function of the lattice coupling $\beta \sim \frac{1}{g^2}$. One can perform two systematic expansions of the lattice action, at small-β (strong coupling) and large-β (weak coupling), and the results from the two cases do not connect smoothly. More sophisticated arguments reveal that there is a critical β_c at which a first-order phase transition (or a crossover) takes place. The large-β regime is smoothly connected to the $g \to 0$ limit, and hence to the original field theory. On the contrary, the small-β region is not. From the point of view of the lattice, the theory defined by small choices of β is perfectly well-defined and might be worth studying per se: the strong-coupling expansion yields the area-law of confinement for the Wilson loop. Unfortunately, from the field-theory perspective this is purely a lattice artifact: all the physics is governed by the scale set by the lattice, and not by the Yang–Mills dynamics. Another interesting example of bulk phase transition, in which the phase-space structure of the lattice theory is more complicated, has been reconsidered recently in the context of $SU(2)$ pure gauge theory with a mixed fundamental-adjoint action for the gauge fields [10].

We find a similar situation in gauge/gravity dualities. We will perform a set of classical gravity calculations in the presence of a boundary that is needed as a UV regulator. The physics will depend on the dynamics represented by the curved background, but also on some boundary-valued *control parameter* which is assumed to have a field-theory origin. The calculations can be done for all possible values of the control parameter, and produce physically sensible results in gravity. However, in special cases there are phase transitions such that only on one side of the phase space it is possible to remove the unphysical cutoff, and recover the dual field theory. On the wrong side of the transition, by contrast, observables are dominated by the cutoff scale. Ultimately this yields new, unexpected bounds on the region of parameter space in gravity which is related to the dual field theory.

We do not develop a systematic study of this feature. We focus on a specific framework and set of problems that are physically interesting, observe under what conditions these bulk transitions appear, and draw conclusions on the physics relevant to the dual field theories.

We consider a class of Type IIB (super-)gravity solutions, generated by a large number of D5-branes wrapping a two-cycle within the base of the conifold [11], which includes the CVMN model [12, 13]. Several subclasses of backgrounds of this type exhibit multi-scale dynamics, and have been used as a starting point to build the dual of technicolor theories [14] which admit a light composite scalar in the spectrum [15, 16] (see also [17]).

Chiral symmetry breaking has been modelled and studied on some of these backgrounds [18–23] by probing them with D7-branes with a special embedding, in analogy with what was done in [24] and [25, 26]. The interest in this set-up arises because the multi-scale dynamics might help in resolving the phenomenological problems (in particular with the S parameter) of models of EWSB obtained within other frameworks [27].

This paper complements the work presented in [28] by completing the analysis to include backgrounds that were not considered there. The two together cover the entirety of supersymmetric wrapped-D5 solutions that do not show bad singular behaviours. With the purpose of illustrating what bulk transitions are, we also study a different class of Type IIB backgrounds (the flavoured Abelian solutions), which have the main advantage of being peculiarly simple.

The paper is organised as follows. In Section II we introduce the general formalism needed in the rest of the analysis. In Section III we provide the reader with all the useful details about the supergravity solutions. In Section IV we compute the D7 embeddings, and explicate what bulk transitions are by means of an accessible example. In Section V we consider the remaining backgrounds in the wrapped-D5 class, and provide a summary of all the results of this paper together with [28]. We conclude in Section VI by critically discussing our findings and suggesting directions for further studies.

II. DISCUSSION.

In this section, we summarise known general results and fix the notation, keeping explicitly the dependence on the UV regulator. Some of the considerations developed here can be found, in different but related contexts, in [28–34]. We then discuss the case in which a certain class of phase transitions occur in the presence of a finite cutoff, which would be missed by a too naive implementation of the renormalisation procedure.

Let us consider the classical system with the action:

$$\mathcal{S} \;=\; \int \mathrm{d}\sigma \, \sqrt{F^2(\rho)\, \phi'^{\,2} + G^2(\rho)\, \rho'^{\,2}}\,, \qquad (1)$$

which describes a curve in the space $(\rho(\sigma), \phi(\sigma))$, with $0 \leq \phi < 2\pi$ and $\rho \geq 0$, and parameterised by the coordinate σ. We assume that the functions F and G are both positive definite and monotonically non-decreasing, which is true in all the following applications. In this way

large values of ρ correspond to short-distance physics in the dual quantum system. We look for solutions that extend to a UV boundary ρ_U in the radial direction. The curve reaches the boundary at two points with angular separation $\bar{\phi}$, and in the limit $\rho_U \to +\infty$ it is orthogonal to the boundary. [1]

There exist several classes of solutions to the equations of motion. The first type is given by $\phi' = 0$ and we refer to it as *disconnected*. It consist of two straight lines extending from ρ_U all the way down into $\rho \to 0$ at a constant angular separation. By replacing into the action, their energy is

$$E_0 \;=\; 2\int_0^{\rho_U} \mathrm{d}\rho\, G(\rho)\,. \tag{2}$$

More interesting solutions have a U-shaped profile, characterised by the value $\hat{\rho}_o > 0$ of the turning point: the solution at $\rho = \hat{\rho}_o$ obeys $\rho'(\sigma)/\phi'(\sigma) = 0$. We refer to these solutions as *connected*.

After deriving the equations of motion, we exploit reparametrization invariance of the action to choose the ansatz $\rho = \sigma$ and hence $\phi = \phi(\rho)$. The connected configurations are described by two symmetric branches joined smoothly at $\hat{\rho}_o$. We define the following functions [28, 33]:

$$V_{eff}^2(\rho,\hat{\rho}_o) \;\equiv\; \frac{F^2(\rho)}{G^2(\rho)}\left(\frac{F^2(\rho)}{F^2(\hat{\rho}_o)}-1\right), \tag{3}$$

$$\mathcal{Z}(\rho) \;\equiv\; \partial_\rho\left(\frac{G(\rho)}{\partial_\rho F(\rho)}\right), \tag{4}$$

and the solution reads

$$\phi(\rho,\hat{\rho}_o) \;=\; \begin{cases} \frac{\bar{\phi}}{2} \;-\; \int_{\hat{\rho}_o}^{\rho} \mathrm{d}\omega\, \frac{1}{V_{eff}(\omega,\hat{\rho}_o)}\,, & \left(x < \frac{\bar{\phi}}{2}\right) \\ \frac{\bar{\phi}}{2} \;+\; \int_{\hat{\rho}_o}^{\rho} \mathrm{d}\omega\, \frac{1}{V_{eff}(\omega,\hat{\rho}_o)}\,, & \left(x > \frac{\bar{\phi}}{2}\right) \end{cases} \tag{5}$$

The angular separation at the boundary and the energy of the configuration are given by

$$\begin{aligned} \bar{\phi}(\hat{\rho}_o) \;&=\; 2\int_{\hat{\rho}_o}^{\rho_U} \mathrm{d}\rho\, \frac{1}{V_{eff}(\rho,\hat{\rho}_o)} \\ &=\; 2\int_{\hat{\rho}_o}^{\rho_U} \mathrm{d}\rho\, \frac{G(\rho)}{F(\rho)}\frac{1}{\sqrt{\frac{F^2(\rho)}{F^2(\hat{\rho}_o)}-1}}\,, \end{aligned} \tag{6}$$

$$\begin{aligned} E(\hat{\rho}_o) \;&=\; 2\int_{\hat{\rho}_o}^{\rho_U} \mathrm{d}\rho\, \frac{\mathrm{d}E}{\mathrm{d}\rho} \\ &=\; 2\int_{\hat{\rho}_o}^{\rho_U} \mathrm{d}\rho\, \frac{F(\rho)G(\rho)}{F(\hat{\rho}_o)}\frac{1}{\sqrt{\frac{F^2(\rho)}{F^2(\hat{\rho}_o)}-1}}\,, \end{aligned} \tag{7}$$

where the last expression has been obtained by replacing the classical solution into the action.

We remind the reader of three important facts about the U-shaped embeddings.

- The function $F(\rho)$ must be positive definite and monotonically increasing for any $\rho > 0$, as visible from the definition of V_{eff} and how it enters the solution to the equations of motion. As we said, this will always be the case in this paper.
- We must find that $\lim_{\rho\to+\infty} V_{eff} = +\infty$, in order for the relevant boundary conditions to be satisfied. Since we choose a parametrisation of the space in which ϕ is compact, we need a stronger condition: the integral giving the asymptotic separation $\bar{\phi}(\hat{\rho}_o)$ must converge.
- The requirement $\mathcal{Z} < 0$ yields a sufficient condition ensuring stability (the absence of tachyonic fluctuations of the classical configuration), and descends from the concavity conditions of the relevant thermodynamic potential. By contrast, if $\mathcal{Z} > 0$ for every $\rho \geq 0$, then in the limit $\rho_U \to +\infty$ all the U-shaped configurations are classically unstable.

Recall the general result

$$\frac{\mathrm{d}E}{\mathrm{d}\bar{\phi}} \;=\; F(\hat{\rho}_o)\,, \tag{8}$$

that does not depend either on whether one takes the limit $\rho_U \to +\infty$ or on the fact that E diverges in this limit and we must add a counterterm. Such a counterterm cannot be dependent on $\hat{\rho}_o$, and hence not on $\bar{\phi}$. This result indicates that $F(\hat{\rho}_o)$ is the effective tension of the one-dimensional object described by $\mathcal{S}$.

We note two important things. First of all, the energy of the disconnected configuration does not depend on $\bar{\phi}$: there is a whole one-parameter class of inequivalent disconnected configurations all of the same energy. Secondly, if $\lim_{\hat{\rho}_o\to 0} F(\hat{\rho}_o) = 0$, then the connected configuration with $\hat{\rho}_o = 0$ is indistinguishable from a disconnected configuration with the same value of $\bar{\phi}$. This allows us to compare the energies of solutions in the two classes, and we can regulate and renormalise them in the same way.

The fact that F is positive-definite, implies that the functions $E(\hat{\rho}_o)$ and $\bar{\phi}(\hat{\rho}_o)$ are both either increasing or decreasing functions. Moreover, since F is monotonically increasing, given two solutions with different values of $\hat{\rho}_o$ but the same value of $\bar{\phi}$, necessarily $\mathrm{d}E/\mathrm{d}\bar{\phi}$ is larger for the solution with larger $\hat{\rho}_o$.

Now, assume that there exist two different branches of connected solutions which, by appropriately varying $\hat{\rho}_o$, approach the point $(\bar{\phi}_1, E_1)$ from the same side, in the space of globally defined quantities. Then, there is a neighbourhood of $(\bar{\phi}_1, E_1)$ where the two branches represent inequivalent solutions for the same values of $\bar{\phi}$. As we argued, the solutions on the branch which is controlled

[1] The presence of a boundary in the space means that we should also add a boundary-localised term to the action. We do not write it explicitly, but implicitly we use it to remove a divergence in the energy of the configurations.

by larger values of $\hat{\rho}_o$ will have larger values of $\mathrm{d}E/\mathrm{d}\bar{\phi}$. Hence, they have lower energy than the configurations with smaller $\hat{\rho}_o$ for $\bar{\phi} < \bar{\phi}_1$, and are thermodynamically favoured, while they have higher energy for $\bar{\phi} > \bar{\phi}_1$, in which case the configurations having smaller $\hat{\rho}_o$ are dominant. This consideration will be useful in order to comment on the numerical results of our analysis.

We are now ready to tackle the main point we want to highlight. The parameter ρ_U is to be understood as a UV-cutoff and we shall choose it to be always much larger than any dynamical scale in the background. We should take the limit $\rho_U \to +\infty$ to recover physical results. Let us make explicit the cutoff dependence of the globally defined quantities $\bar{\phi}(\hat{\rho}_o, \rho_U)$ and $E(\hat{\rho}_o, \rho_U)$. For large values of $\hat{\rho}_o$ there are two possible orders of limits:

a) we could first fix $\hat{\rho}_o$, take the limit $\rho_U \to +\infty$, and thereafter vary $\hat{\rho}_o$

$$\bar{\phi}_a \equiv \lim_{\hat{\rho}_o \to +\infty} \lim_{\rho_U \to +\infty} \bar{\phi}(\hat{\rho}_o, \rho_U)\,, \tag{9}$$

$$\bar{E}_a \equiv \lim_{\hat{\rho}_o \to +\infty} \lim_{\rho_U \to +\infty} \Big(E(\hat{\rho}_o, \rho_U) - E_0(\rho_U) \Big)\,, \tag{10}$$

b) alternatively, we could first keep fixed the UV cutoff, and study the system for varying $\hat{\rho}_o$, and only afterwards take the limit $\rho_U \to \infty$

$$\bar{\phi}_b \equiv \lim_{\rho_U \to +\infty} \lim_{\hat{\rho}_o \to +\rho_U} \bar{\phi}(\hat{\rho}_o, \rho_U) = 0\,, \tag{11}$$

$$\bar{E}_b \equiv \lim_{\rho_U \to +\infty} \lim_{\hat{\rho}_o \to +\rho_U} \Big(E(\hat{\rho}_o, \rho_U) - E_0(\rho_U) \Big)\,. \tag{12}$$

In most cases, the two limits commute, since frequently $\bar{\phi}_a = 0 = \bar{\phi}_b$. Notice that to calculate $\bar{E}$ from E, we subtracted the divergent $E_0(\rho_U)$, and in this scheme the disconnected solutions always have vanishing energy.

The potential problem arises when $\bar{\phi}_a$ is finite. There exist many examples of this, some of which are well known (for instance the D3-D7 system [8]). Convergence of the limits defining $\bar{\phi}_a$ means that, at least for $\hat{\rho}_o$ large enough, $\lim_{\rho_U \to +\infty} \bar{\phi}(\hat{\rho}_o, \rho_U)$ becomes effectively independent of $\hat{\rho}_o$. By contrast, if we compute $\bar{\phi}_b$, for $\hat{\rho}_o$ large enough the angular separation will first tend to converge towards $\bar{\phi}_a$ while increasing $\hat{\rho}_o$, but when the configuration becomes short and $\hat{\rho}_0$ is taken close to ρ_U, suddenly the angular separation starts to decrease and eventually vanish. The resulting *short* configurations keep existing for any finite choice of ρ_U, but they probe only a very narrow region close to the boundary. For this reason, these configurations cannot be seen if we take the ordering as in case a) above.

The question is then: are these short connected solutions, that are always localised in the proximity of the regulating ρ_U, physical configurations, or a mere artefact of the regulation procedure? Equivalently, which of the cases a) and b) yields physically sensible results? The answer is that the short configurations are necessary in order to cure an otherwise fatal pathology in the free energy, which may become discontinuous as a function of the control parameter $\bar{\phi}$ if we follow procedure a). Hence we must use procedure b). We will see explicit examples of this discontinuity in Section V.

Short configurations are of no interest per se, because they do not probe the geometry of the space described by the functions F and G, and hence are unrelated to the dual field theory. Unfortunately, they become thermodynamically favoured when $\bar{\phi} < \bar{\phi}_a$, inducing a phase transition. For all practical purposes this amounts to the existence of a physical lower bound on $\bar{\phi}$, below which the dynamics is dominated by cutoff effects. This phenomenon is reminiscent of *bulk* phase transitions on the lattice, and we adopt the convention of calling it by the same name.

Let us now explain why procedure b) yields a phase-transition when $\bar{\phi}_a > 0$. We first fix a large value of ρ_U. When varying $\hat{\rho}_o$ in the region where the angular separation is approaching $\bar{\phi}_a$, there are two possibilities. If $\mathrm{d}\bar{\phi}/\mathrm{d}\hat{\rho}_o < 0$, nothing special happens: $\bar{\phi}_b$ will decrease and approach $\bar{\phi}_a$, until $\hat{\rho}_o$ becomes so close to ρ_U that the configuration is short, and $\bar{\phi}_b$ keeps decreasing monotonically. On the other hand, if $\mathrm{d}\bar{\phi}/\mathrm{d}\hat{\rho}_o > 0$ for some large $\hat{\rho}_o$, by increasing $\hat{\rho}_o$ the sign of this derivative will have to change, since ultimately $\bar{\phi}_b$ vanishes. This signals a turning point in the $(\bar{\phi}_b, E_b)$ plane, giving rise to two different branches of solutions. As we said, in the proximity of the turning point the derivative $\mathrm{d}E/\mathrm{d}\bar{\phi}$ will be larger for the branch with larger $\hat{\rho}_0$. This is the branch of the short configurations, which is hence thermodynamically favoured.

By looking at E_b one sees that the short solutions have negative energy, which would diverge for $\rho_U \to +\infty$: they dominate the dynamics atop any other configuration. However, this branch does not exist for $\bar{\phi} > \bar{\phi}_a$. By contrast the disconnected solution always exists and has vanishing energy, which means that at $\bar{\phi} = \bar{\phi}_a$ there must be a phase transition, with either the disconnected or a connected solution becoming the minimum of the energy in the physical region $\bar{\phi} > \bar{\phi}_a$.

Let us finally explain why procedure a) is potentially problematic. We can think of this setup as the saddle-point approximation of a statistical mechanics system, and interpret $\bar{E}$ as the Gibbs free energy, expressed in terms of the external control parameter $\bar{\phi}$. In the way we computed it earlier, $\bar{E}(\bar{\phi})$ is in general multivalued, and the approximation requires us to retain only its global minimum, when several different configurations sharing the same $\bar{\phi}$ exist. The subtle point is that the resulting $\bar{E}(\bar{\phi})$ must be continuous, and hence (global) minimization must be carried out before taking the $\rho_U \to +\infty$ limit.

The drawback of procedure a) is that, while the results it yields for all other branches agree with procedure b), it completely suppresses the short configurations. Since such solutions have the lowest energy (when $\bar{\phi}_a > 0$), removing them may result in unphysical discontinuities of the Gibbs free energy. Consequently, procedure a) does not provide a good approximation of the free energy.

In computing any physical observables, including the free energy — but also the separation $\bar{\phi}$ itself — one must first find the global minimum of the energy, only afterwards apply subtractions and finally take the $\rho_U \to +\infty$ limit. Ultimately, following procedure b) ensures that $\bar{E}(\bar{\phi})$ is always continuous, provides a natural explanation for the bound $\bar{\phi} > \bar{\phi}_a$, and does not affect in any way phenomena taking place in the physical region above this bound.

III. THE WRAPPED-D5 SYSTEM.

We focus on a special, large class of Type IIB backgrounds which we refer to as the *wrapped-D5* system. We do not repeat all the details about the general solutions, which can be found elsewhere [35, 36]. We follow closely the notation in the recent paper [28] and only mention those element that are directly relevant for the following sections.

The system is a truncation of Type IIB supergravity that contains only gravity, the dilaton Φ and the RR three-form F_3. The internal part of the metric is related to $T^{1,1}$, and we write it in terms of the following vielbein:

$$\begin{aligned} e_1 &= -\sin\theta\,\mathrm{d}\phi\,, \quad e_2 = \mathrm{d}\theta\,,\\ e_3 &= \cos\psi\,\sin\tilde{\theta}\,\mathrm{d}\tilde{\phi} - \sin\psi\,\mathrm{d}\tilde{\theta}\,,\\ e_4 &= \sin\psi\,\sin\tilde{\theta}\,\mathrm{d}\tilde{\phi} + \cos\psi\,\mathrm{d}\tilde{\theta}\,,\\ e_5 &= \mathrm{d}\psi + \cos\theta\,\mathrm{d}\phi + \cos\tilde{\theta}\,\mathrm{d}\tilde{\phi}\,, \end{aligned} \tag{13}$$

where the range of the five angles is $0 \le \theta\,,\, \tilde{\theta} < \pi\,,\, 0 \le \phi\,,\, \tilde{\phi} < 2\pi\,,\, 0 \le \psi < 4\pi$. We assume that the functions defining the background depend only on the radial coordinate ρ. The metric (in Einstein frame) reads

$$\begin{aligned} \mathrm{d}s_E^2 &= \alpha' g_s\, e^{\Phi/2}\Big[(\alpha' g_s)^{-1} dx_{1,3}^2 + ds_6^2\Big],\\ \mathrm{d}s_6^2 &= e^{2k} d\rho^2 + e^{2h}(e_1^2 + e_2^2)\\ &\quad + \frac{e^{2g}}{4}\Big((e_3 + a\,e_1)^2 + (e_4 + a\,e_2)^2\Big) + \frac{e^{2k}}{4} e_5^2\,. \end{aligned} \tag{14}$$

The string-frame metric is $\mathrm{d}s^2 = e^{\frac{\Phi}{2}}\mathrm{d}s_E^2$, we fix the coupling to $\alpha' g_s = 1$, and ignore the non-vanishing F_3 (see for instance [36]).

The system of BPS equations derived using this ansatz can be reorganized in terms of convenient functions [36]:

$$\begin{aligned} 4\,e^{2h} &= \frac{P^2 - Q^2}{P\cosh\tau - Q}\,, \qquad e^{2g} = P\cosh\tau - Q\,,\\ e^{2k} &= 4\,Y\,, \qquad\qquad a = \frac{P\sinh\tau}{P\cosh\tau - Q}\,, \end{aligned} \tag{15}$$

such that it reduces to a single decoupled second-order equation for the function $P(\rho)$ that takes the form

$$P'' + P'\left(\frac{P'+Q'}{P-Q} + \frac{P'-Q'}{P+Q} - 4\coth(2\rho - 2\rho_0)\right) = 0\,, \tag{16}$$

where the prime refers to derivatives with respect to ρ. All other functions can be read from

$$\begin{aligned} Q &= (Q_0 + N_c)\cosh\tau + N_c\,(2\rho\cosh\tau - 1)\,,\\ Y &= \frac{P'}{8}\,, \qquad\qquad \cosh\tau = \coth(2\rho - 2\rho_0)\,,\\ e^{4\Phi} &= \frac{e^{4\Phi_0}\cosh(2\rho_0)^2}{(P^2 - Q^2)Y\sinh^2\tau}\,. \end{aligned} \tag{17}$$

We refer to Eq. (16) as the *master equation*. In the following we take the end of space to be at $\rho_0 = 0$ and tune $Q_0 = -N_c$. The remaining constant Φ_0 is a free parameter of little physical meaning, and we set $\Phi_0 = 0$. The generic solution for P depends on two integration constants.

The master equation has to be solved numerically, the only solution known in closed form being the famous CVMN solution [12, 13]:

$$\hat{P} = 2N_c\rho\,. \tag{18}$$

All other solutions with regular P are approximated by

$$P_a \simeq \sup\Big\{\, c_0\,,\, 2N_c\rho\,,\, 3c_+ e^{4\rho/3}\Big\}\,, \tag{19}$$

where c_0 and c_+ are two integration constants. When c_0 effectively vanishes, for small ρ the solution is best approximated by the expansion [36]:

$$P_\ell = h_1\rho + \frac{4h_1}{15}\left(1 - \frac{4N_c^2}{h_1^2}\right)\rho^3 + \mathcal{O}(\rho^5)\,, \tag{20}$$

in which $h_1 \ge 2N_c$ is the remaining integration constant. The value $h_1 = 2N_c$ reproduces exactly the CVMN solution. Discussions of these backgrounds can be found elsewhere [28, 36, 37]. In particular, in [37] one finds the details about the relation between these backgrounds and the baryonic branch [38] of the Klebanov–Strassler system [39] and other backgrounds within the Papadopoulos–Tseytlin ansatz [40] and its generalisation [41], via the rotation (or U-duality) procedure introduced and studied in [42–44].

A. Flavored Abelian solutions.

We introduce a related class of Type IIB solutions, which we refer to as Abelian [36]. Some of the background functions (related to the gaugino condensate) are omitted, in particular the function a, which is related to the $SU(2)$-twisting from which the distinction between Abelian and non-Abelian backgrounds originates [13].

The Abelian solutions can be obtained by replacing $\tau = 0$ in the earlier ansatz. The only delicate piece is the dilaton, that in our conventions reads

$$e^{4\Phi} = \frac{e^{4\Phi_0} e^{4\rho}}{4(P^2 - Q^2)Y}\,. \tag{21}$$

A further modification of the system consists in introducing flavor in the form of N_f smeared D5-branes. The details can be found in [35, 36]. The background metric obeys the same ansatz. The only modifications appear in the functions Q and Y and in the master equation:

$$Y \;=\; \frac{P'+N_f}{8}\,, \qquad\qquad Q \;=\; Q_o + N_c - \frac{N_f}{2} + \left(N_c - \frac{N_f}{2}\right)(2\rho-1)\,, \tag{22}$$

$$0 \;=\; P'' + (P'+N_f)\left(\frac{P'+Q'+2N_f}{P-Q} + \frac{P'-Q'+2N_f}{P+Q} - 4\right). \tag{23}$$

For $N_f = 2N_c$, there exists the exact solution [36]

$$Q \;=\; \frac{3N_c}{4}\,, \qquad\qquad P \;=\; \frac{9N_c}{4} + c_+\, e^{4\rho/3}\,, \tag{24}$$

with $c_+ \geq 0$ a constant. The end-of-space in the IR is now located at $\rho \to -\infty$. Indeed, for $c_+ = 0$ all the background functions become constant, with the exception of the linear dilaton. With abuse of language, we call it *scale invariant*.

IV. D7 EMBEDDING.

We embed a probe-D7 [18, 25, 26] so that it fills the four Minkowski coordinates and the internal three-manifold $(\tilde\theta, \tilde\phi, \psi)$. Since B_2 is trivial, we set the gauge field on the brane to $\mathcal{F}_2 = 0$. We treat ρ, ϕ and θ as functions of the embedding coordinate σ. Integrating the rest of the angular variables, the DBI action $\mathcal{S}_{D7} \propto \int \mathrm{d}^8x\,\sqrt{-\tilde g_8}\,e^{-\Phi}$ becomes

$$\mathcal{S}_{D7} \;\propto\; \int \mathrm{d}^4x\,\mathrm{d}\sigma\,\sqrt{e^{4g+4k+6\Phi}\rho'^{\,2} + e^{4g+2k+2h+6\Phi}\left(\theta'^{\,2} + \sin^2\theta\,\phi'^{\,2}\right)}\,. \tag{25}$$

The function a disappears from this expression, so that we can use the same formalism to deal both with Abelian and non-Abelian backgrounds. For symmetry reasons, without loss of generality we choose configurations at the equator $\theta = \frac{\pi}{2}$. Finally, the action takes the form of $\mathcal{S}$ presented in Eq. (1), provided we make the identifications

$$F^2 \;=\; e^{4g+2k+2h+6\Phi}\,, \qquad\qquad G^2 \;=\; e^{4g+4k+6\Phi}\,. \tag{26}$$

A. Flavored Abelian backgrounds.

We consider the flavoured Abelian solution, which is simple enough that we can perform most of the computations analytically, serving for illustrational purposes. The background functions read:

$$\begin{aligned} F^2 \;&=\; \frac{e^{6\rho}}{2}\sqrt{\frac{P-Q}{2(P'+N_f)(P+Q)}} \\ &=\; \frac{\sqrt{3}\,e^{6\rho}}{4\sqrt{6+2c_+\,e^{4\rho/3}}}\,, \end{aligned} \tag{27}$$

$$\begin{aligned} G^2 \;&=\; \frac{e^{6\rho}}{(P+Q)^2}\sqrt{\frac{(P'+N_f)(P^2-Q^2)}{2}} \\ &=\; \frac{e^{6\rho}}{\sqrt{6}}\,\frac{3+2c_+\,e^{4\rho/3}}{(3+c_+\,e^{4\rho/3})^{3/2}}\,, \end{aligned} \tag{28}$$

where we replaced the special solutions presented earlier, and fixed $N_c = 1$. Both F and G diverge at large-ρ, as anticipated.

We start from the case $c_+ = 0$, for which

$$F^2 \;=\; \frac{e^{6\rho}}{4\sqrt{2}}\,, \qquad\qquad G^2 \;=\; \frac{e^{6\rho}}{3\sqrt{2}}\,. \tag{29}$$

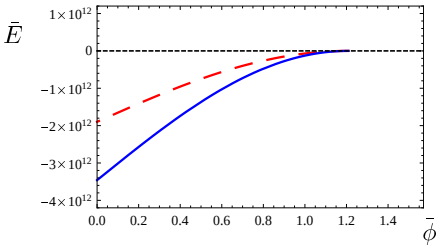

FIG. 1: Dependence of the subtracted energy $\bar{E}$ on the angular separation $\bar{\phi}$, computed for the scale-invariant solutions of the Abelian flavoured system. We show the disconnected configuration (black short-dashed), together with the connected configurations computed with fixed ρ_U by varying $\hat{\rho}_o$. The (red) long-dashed curve has $\rho_U = 9.8$, while the (blue) continuous curve was computed with $\rho_U = 10$.

As a result, we find

$$V_{eff}^2 = \frac{3}{4}\left(-1 + e^{6(\rho-\hat{\rho}_0)}\right), \tag{30}$$

$$\frac{\mathrm{d}E}{\mathrm{d}\rho} = \frac{1}{2^{1/4}\sqrt{3}}\frac{e^{6\rho}}{\sqrt{e^{6\rho}-e^{6\hat{\rho}_o}}}, \tag{31}$$

$$\mathcal{Z} = 0\,. \tag{32}$$

We immediately see that the conditions we outlined for F and V_{eff} are satisfied. The condition for $\mathcal{Z}$ is more subtle: its vanishing is a limiting case.

Integrating one obtains the energy and asymptotic separation

$$\bar{\phi}(\hat{\rho}_o,\rho_U) = \frac{4}{3\sqrt{3}}\arctan\sqrt{-1+e^{6(\rho_U-\hat{\rho}_o)}}, \tag{33}$$

$$E(\hat{\rho}_o,\rho_U) = \frac{2^{3/4}}{3\sqrt{3}}\sqrt{e^{6\rho_U}-e^{6\hat{\rho}_o}}, \tag{34}$$

$$E_0 = \frac{2^{3/4}}{3\sqrt{3}}e^{3\rho_U}, \tag{35}$$

where the lower end of the integral yielding E_0 is the end-of-space $\rho \to -\infty$.

Following procedure a), i. e. if we first take the limit in which we remove the cutoff, we see the emergence of a peculiar situation. Namely, independently of $\hat{\rho}_o$, we find that

$$\lim_{\rho_U\to+\infty}\bar{\phi}(\hat{\rho}_o,\rho_U) = \frac{2\pi}{3\sqrt{3}} \equiv \bar{\phi}_a\,, \tag{36}$$

$$E(\hat{\rho}_o,\rho_U) - E_0(\rho_U) = -\frac{e^{6\hat{\rho}_o-3\rho_U}}{2^{1/4}3\sqrt{3}} + \cdots \to 0\,. \tag{37}$$

There exists only one point in the $(\bar{\phi}_a, \bar{E}_a)$ plane. All the connected configurations admissible as solutions, for any $\hat{\rho}_o$, yield the same result in terms of physical quantities. To this, one has to add the disconnected configurations:

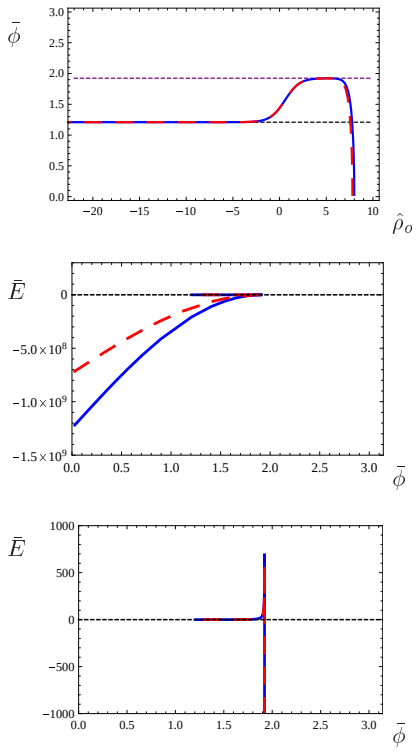

FIG. 2: Numerical study in the Abelian flavoured case with $c_+ = 1 = N_c$, and $N_f = 2$. The (blue) continuous curves show the results for the connected configurations with $\rho_U = 8$, and the (red) long-dashed curves for $\rho_U = 7.8$. The top panel shows the dependence of $\bar{\phi}$ on $\hat{\rho}_0$ in the two cases, the short-dashed lines represent the asymptotic values $\bar{\phi} = 2\pi/3\sqrt{3}$ (black) and $\bar{\phi} = \sqrt{6}\pi/4$ (purple). The middle plot shows the dependence of the subtracted energy $\bar{E}$ on $\bar{\phi}$, with the short-dashed line (black) representing the disconnected solution. The bottom panel shows a detail of the middle one.

given that $\lim_{\rho\to-\infty} F(\rho) = 0$, the limit $\hat{\rho}_o \to -\infty$ is indistinguishable from the disconnected configuration.

For any choice of $\bar{\phi}$, there exists the disconnected configuration, that has constant energy. For the special value $\bar{\phi} = \bar{\phi}_a$ there exists a whole other branch of connected solutions, again with the same energy.

However, following procedure b) we obtain another branch of configurations, the short connected ones. We display in Fig. 1 the behaviour of the subtracted energy $\bar{E} = E - E_0$, as a function of $\bar{\phi}$, for two different values of the cutoff $\rho_U = 9.8$ and $\rho_U = 10$, compared with the disconnected configuration. [2]

[2] Here and in the following, the plots have been made by fixing a large value of the UV cutoff, and then subtracting the energy of the disconnected solution for the same ρ_U. The choice of cutoff

Both from the analytical results, and from the figure, we can see four important things. First, the short configurations have lower energy than the disconnected ones, and hence are always dominant for $\bar{\phi} < \bar{\phi}_a$. Secondly, rather than decoupling when $\rho_U \to +\infty$, the energy of the short configurations keeps decreasing, so that they become more dominant the larger the value of ρ_U. Third, the limit $\bar{\phi} \to \bar{\phi}_a$ coincides with the taking the limit $\hat{\rho}_0 \to -\infty$. Since in this limit $F(\hat{\rho}_o) \to 0$, the branch of short configurations joins smoothly with the disconnected one, giving rise to a second-order phase transition. Finally, the short connected solutions are concave functions of $\bar{\phi}$, which means that they are classically stable.

The algebra is simple enough that we can solve for $\hat{\rho}_o$ in $\bar{\phi}(\hat{\rho}_o, \rho_U)$, and replace into the subtracted energy:

$$\bar{E}(\bar{\phi}, \rho_U) \;=\; \frac{2^{3/4}}{3\sqrt{3}}\, e^{3\rho_U} \left(\sin\left(\frac{3\sqrt{3}}{4}\bar{\phi}\right) - 1 \right), \quad (38)$$

$$\partial_{\bar{\phi}} \bar{E}(\bar{\phi}, \rho_U) \;=\; \frac{1}{2^{5/4}}\, e^{3\rho_U} \cos\left(\frac{3\sqrt{3}}{4}\bar{\phi}\right), \quad (39)$$

$$\partial^2_{\bar{\phi}} \bar{E}(\bar{\phi}, \rho_U) \;=\; -\frac{3\sqrt{3}}{2^{1/4}8}\, e^{3\rho_U} \sin\left(\frac{3\sqrt{3}}{4}\bar{\phi}\right). \quad (40)$$

In the limit $\bar{\phi} \to \bar{\phi}_a$, we find $\bar{E} = 0 = \partial_{\bar{\phi}} \bar{E}$: the free energy is continuous and has continuous derivative, but $\partial^2_{\bar{\phi}} \bar{E} \propto e^{3\rho_U} \neq 0$, so the system exhibits a second-order phase transition.

We now consider the full solution (24) and set $c_+ = 1$ for convenience. In the IR the geometry reproduces the previous results. In the UV new effects appear. Fig. 2 shows the numerical study of the system, for which we used the cutoffs $\rho_U = 7.8$ and $\rho_U = 8$.

Plugging (24) into (3) and (4), it can be seen that V_{eff} diverges when $\rho \to +\infty$. However, we encounter a problem with the function $\mathcal{Z}$, which is positive definite. We expect the concavity condition to be violated, and hence the long connected configurations are classically unstable. This is visible in the bottom panel of Fig. 2, where the branch of connected, long solutions, which always have positive energy, has the wrong convexity.

If we were to restrict our attention to connected configurations, and apply procedure a), thus ignoring the short configurations, we would solely find the branch with positive $\bar{E}$. This would pose two puzzling results. The first is that these solutions are classically unstable. The second is that these configurations only exist provided

$$\frac{2\pi}{3\sqrt{3}} < \bar{\phi} < \frac{\sqrt{6}}{4}\pi\,. \quad (41)$$

The asymptotic values are reached for $\hat{\rho}_o \to -\infty$ in the case of the lower bound, and for $\hat{\rho}_o$ asymptotically large, but still far from the UV cutoff, in the case of the upper bound. The presence of the lower bound is not a surprise: we have the same geometry as before, in the deep IR, and hence brane configurations that extend very deep in the IR effectively behave as in the scale-invariant case.

The upper bound comes from the drastic modification of the geometry induced in the far-UV by $c_+ > 0$. We can approximate the geometry here by setting $Q = 0 = N_f$ and $P = e^{4\rho/3}$. By replacing in the various functions needed, we find

$$\bar{\phi}(\hat{\rho}_o, \rho_U) \;=\; \sqrt{\frac{3}{2}} \arctan \sqrt{-1 + e^{\frac{16}{3}(\rho_U - \hat{\rho}_o)}}\,, \quad (42)$$

which for $\rho_U \to +\infty$ converges to $\bar{\phi}(\hat{\rho}_o, \rho_U) \to \sqrt{6}\pi/4$.

On the basis of the general considerations we are making, we expect that procedure b) reveals another branch of solutions, which exists for any value $\bar{\phi} < \bar{\phi}_a = \sqrt{6}\pi/4$. This can be seen in the figure, which also shows that the short connected configurations become more dominant when the UV cutoff is taken to be large.

The transition between short and disconnected configurations is first order, contrary to the scale-invariant case. Another distinction is that long connected configurations do not have the same energy as the disconnected ones. Long connected solutions, besides being classically unstable, always have energy larger than the short connected or the disconnected solutions.

The conclusion is that in this system there is now a bound $\bar{\phi} > \sqrt{6}\pi/4$ on the control parameter. Furthermore, the disconnected configuration is always the one physically realised, so this type of set-up cannot be used to describe chiral symmetry breaking.

V. CHIRAL SYMMETRY BREAKING IN THE WRAPPED-D5 SYSTEM.

We move now to the main topic of the paper, that is, the unflavored, non-Abelian solutions to the wrapped-D5 system, for which P_a or P_ℓ provide an approximation of the background. There exist only two admissible UV-asymptotic expansions: either P is linear with ρ, or exponentially growing. In the former case, $\bar{\phi}$ converges towards a vanishing value for connected configurations when $\hat{\rho}_o$ is large. All possible backgrounds of this class are not affected by bulk transitions and the existence of a phase transition between connected and disconnected configurations has been studied in [28].

We hence focus on solutions for which the asymptotic behaviour is dominated by the exponential growth of P. There are several subclasses, depending on the IR behaviour of the background.

is large enough, that changing it to even larger values, has no appreciable effect on the side of the phase transition connected to the gravity dual. On the other side of the bulk transition, by looking at increasing values of the cutoff, one sees that the energy eventually diverges to $-\infty$. The plots of the different values of ρ_U (see Fig. 1 and Fig. 2) are used to illustrate this.

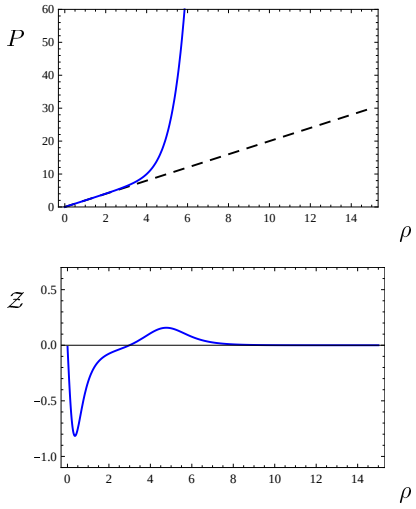

FIG. 3: Example of a numerical solution to the non-Abelian system, with IR asymptotics given by P_ℓ. The top panel shows the function P, the bottom panel the function $\mathcal{Z}$. We set $N_c = 1 = e^{\Phi_o}$.

A. Non-Abelian solutions and the baryonic branch.

We start with the one-parameter family of regular backgrounds with $c_0 = 0$, i.e. those that are controlled by a linear P for $\rho < \bar{\rho}$ and exponential for $\rho > \bar{\rho}$. It has been noted in [42–44] that after U-duality these reproduce the baryonic branch of the Klebanov–Strassler system. With abuse of language we refer to them as the baryonic branch, although strictly speaking they agree with it only in the IR. In the deep IR they are well approximated by the expansion P_ℓ. The parameter c_+ in the UV expansion controls the scale $\bar{\rho}$ below which the dimension-two baryonic VEV becomes important.

We display in Fig. 3 an example in this class, with $\bar{\rho} \simeq 3$ (obtained with $h_1 = 2.004$). The figure shows the functions P and $\mathcal{Z}$. The necessary conditions outlined in the general discussion on the functions F and V_{eff} are satisfied, but the function $\mathcal{Z}$ is not negative definite. In particular, for $\rho > \bar{\rho}$ it becomes positive, indicating that we expect the arising of an instability. We show in Fig. 4 the results of the numerical study of the background in Fig. 3.

In this case there is a physical end-of-space in the IR, which we set to $\rho_0 = 0$. In this region, the geometry resembles that of the CVMN solution, and indeed as $\hat{\rho}_o \to 0$, the separation tends to $\bar{\phi} \to \pi$, while the energy $\bar{E} \to 0$. Moreover, $F(0) = 0$ implies that $\mathrm{d}\bar{E}/\mathrm{d}\bar{\phi} = 0$. Hence, the connected configurations that extend deep into the IR are the equilibrium solutions, having the correct concavity and energy lower than the disconnected ones. This situation is common to the whole class with IR asymptotics given by P_ℓ.

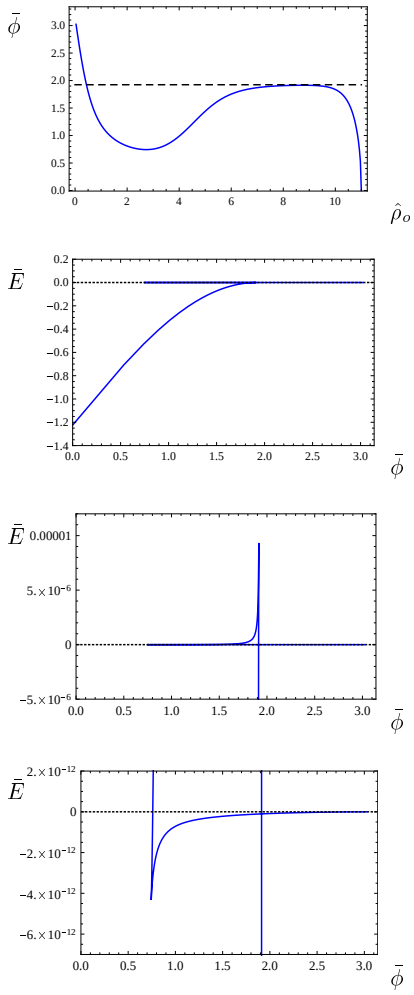

FIG. 4: Study of the embedding for the background in Fig. 3. The continuous (blue) curves are obtained for $\rho_U = 11$. The top panel shows the functional dependence of $\bar{\phi}$ on $\hat{\rho}_o$. The dashed (black) line is the asymptotic value $\bar{\phi} = \sqrt{6}\pi/4$. The other panels show the dependence of $\bar{E}$ on $\bar{\phi}$, with the dashed (black) line representing the disconnected solutions.

Fig. 4 shows details of the $(\bar{\phi}, \bar{E})$ plane, showing the four branches of solutions, their concavity, and the range of $\bar{\phi}$ for which they exist. The branch that reaches the maximal separation $\bar{\phi} \to \pi$ is clearly visible in the last panel of the figure. It exists for $\bar{\phi} > \bar{\phi}_1$, determined by the value of $\bar{\rho}$ (in the figure, $\bar{\phi}_1 \simeq 0.7$). A second branch is visible in the third panel from the top. It has the wrong concavity, and hence represents unstable classical solutions that probe the geometry no further than $\bar{\rho}$. It exists only in the range $\bar{\phi}_1 < \bar{\phi} < \bar{\phi}_a = \sqrt{6}\pi/4$. Solutions along this branch always have energy larger than the first

class. The third class of solutions are the disconnected ones.

If only these three classes existed, we would be faced with a serious problem. Interpreting the minimum of $\bar{E}$ as the free energy $\mathcal{G}$, we would be left with a discontinuity in $\mathcal{G}$ as a function of $\bar{\phi}$. This is the result one gets by applying procedure a) while regulating the calculations. This example clearly shows that it yields nonsensical results. Procedure b) allows us to retain a fourth branch consisting of short configurations localized in the vicinity of the UV cutoff. How close can be seen in the right-hand side of the top panel in Fig. 4. This is the branch that reaches $\bar{\phi} \to 0$, apparent in the second panel from the top of the figure. It has the correct concavity, large values of $\mathrm{d}\bar{E}/\mathrm{d}\bar{\phi}$ (actually divergent in the $\rho_U \to +\infty$ limit) and exists only for $\bar{\phi} < \bar{\phi}_a$. Whenever present it is always the minimum of $\bar{E}$.

The conclusion is that a first-order bulk phase transition takes place at $\bar{\phi} = \bar{\phi}_a$. For smaller values of the control parameter, the equilibrium configurations are the short ones, that do not probe the interior of the geometry. For larger values the equilibrium is reached by long connected configurations with $\hat{\rho}_o < \bar{\rho}$.

An alternative phrasing is that there exists a physical bound on the control parameter $\bar{\phi} > \bar{\phi}_a$. For smaller values it is not possible to interpret the results in dual field-theoretic terms.

Notice that, for any choice of $\bar{\rho}$, the turning point in the $(\bar{\phi}, \bar{E})$ plot is always situated at $\bar{\phi}_1 < \bar{\phi}_a$. This is of crucial importance, since it proves that $\bar{E}$ is continuous. The position of the turning point depends on the value of $\bar{\rho}$, or equivalently h_1. It moves towards $\bar{\phi}_1 \to 0$ in the limit $\bar{\rho} \to +\infty$ (corresponding to $h_1 \to 2$), while $\bar{\phi}_1 \to \bar{\phi}_a$ when $h_1 \to +\infty$. The latter is the limit in which the baryonic VEV is suppressed and the rotation allows us to reconstruct the Klebanov–Strassler solution [37, 44].

We checked numerically that even for $h_1 \simeq 40000$ the turning point is at $\bar{\phi}_1 < \bar{\phi}_a$. There is a simple reason for this: solutions with $\hat{\rho}_o \gg \bar{\rho}$ still have $\mathrm{d}\bar{E}/\mathrm{d}\bar{\phi} > 0$, which requires that the turning point verifies $\bar{\phi}_1 < \bar{\phi}_a$.

B. Walking solutions on the baryonic branch.

We now consider a non-vanishing P in the IR, that is $P \simeq c_0$ for small values of ρ, while in the far UV it is again exponentially growing as $P \simeq 3\, c_+ e^{4\rho/3}$. There are two integration constants, c_0 and c_+, which are chosen such that there is an intermediate range where P approximates the CVMN solution.

In Fig. 5, we show an example of P in this class. As can be seen, there are now three physical scales: the end of space $\rho_0 = 0$, a scale ρ_* below which P is approximately constant (we call this the *walking* region), and a scale $\bar{\rho}$ above which P is exponentially growing. In the range

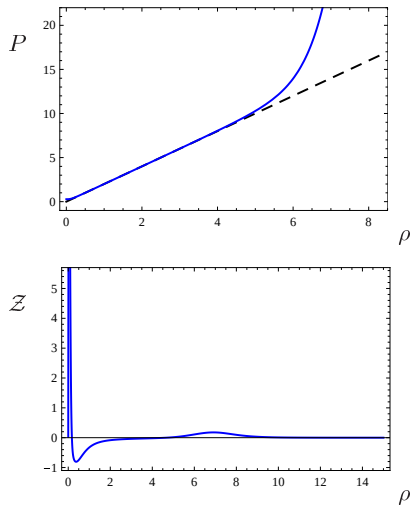

FIG. 5: Example of a numerical solution to the non-Abelian system, with IR asymptotics given by a constant $P \simeq c_0$. The top panel shows the function P, the bottom panel the function $\mathcal{Z}$. We set $N_c = 1 = e^{\Phi_o}$. Notice how the scale ρ_* is quite small.

$\rho_* < \rho < \bar{\rho}$ we have that $P \simeq \hat{P}$. [3]

Now $\mathcal{Z}$ changes sign twice: deep in the IR and far in the UV, $\mathcal{Z} > 0$, which suggests that probe branes extending only in the far UV, or very deep in the IR, are classically unstable. From the figure we identify $\bar{\rho} \simeq 4$ and $\rho_* \simeq 0.2$ with the zeros of $\mathcal{Z}$.

We embed D7-branes as explained in Section IV. The result is illustrated in Fig. 6, where we performed the calculations with UV cutoff $\rho_U = 10.1$. First of all, for $\rho > \rho_*$ the background is essentially identical to the baryonic branch of the previous subsection. Unsurprisingly the probes behave in the same way as long as $\hat{\rho}_o > \rho_*$. For branes that extend very close to the end of space, with $\hat{\rho}_o < \rho_*$, the aforementioned classical instability manifests itself in the presence of a fifth branch, along which the function $\bar{E}(\bar{\phi})$ has the wrong concavity. From the top panel of the figure one sees that there is a range of $\bar{\phi}$ where we have five different branches of classical solutions (including the disconnected ones) yielding a richer structure of phase transitions.

The short connected configurations dominate the dynamics for $\bar{\phi} < \bar{\phi}_a$. Increasing $\bar{\phi}$, there is a bulk phase transition, and in the range $\bar{\phi}_a < \bar{\phi} < \bar{\phi}_c$ the connected configurations that we saw taking over in the

[3] Unfortunately, there is neither a closed relation between c_0 and c_+ and the scales, nor an easy way to extract their values from the numerics. Nevertheless, variation in those parameters do not show qualitative changes in the features we uncover other than the ones we comment.

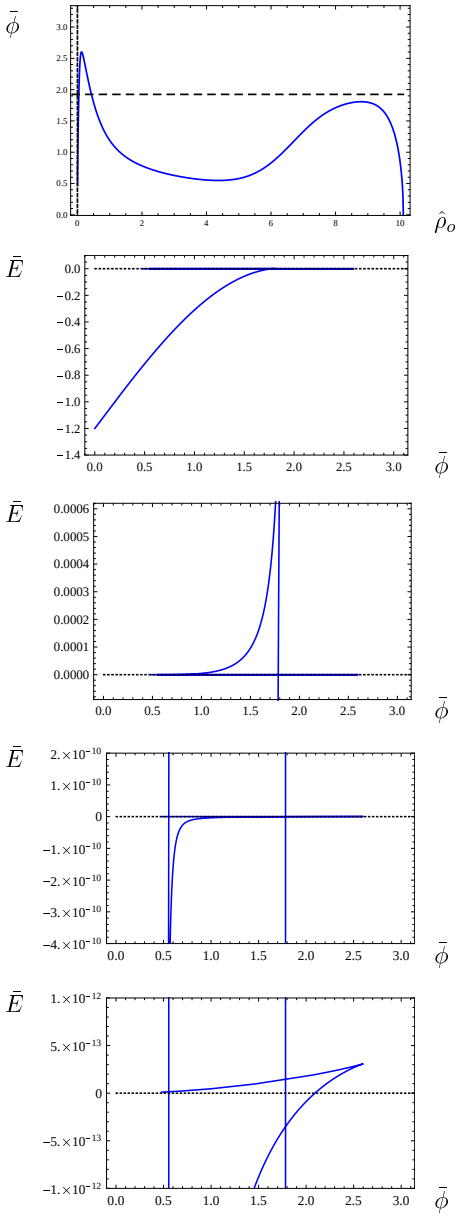

FIG. 6: Study of the embedding for the background in Fig. 5. The continuous (blue) curves are obtained for $\rho_U = 10.1$. The top panel shows the functional dependence of $\bar{\phi}$ on $\hat{\rho}_o$. The long dashed (black) line is the asymptotic value $\bar{\phi} = \sqrt{6}\pi/4$ and the short dashed (black) line represents the disconnected solutions. The other panels show the dependence of $\bar{E}$ on $\bar{\phi}$.

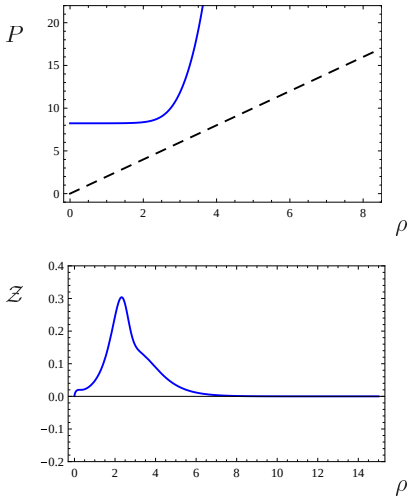

FIG. 7: Example of a numerical solution to the non-Abelian system, with IR asymptotics given by a constant $P \simeq c_0$. The top panel shows the function P, the bottom panel the functions $\mathcal{Z}$. We set $N_c = 1 = e^{\Phi_o}$.

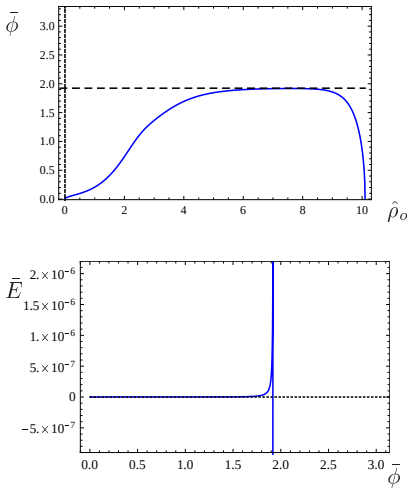

FIG. 8: Study of the embedding for the background in Fig. 7. The continuous (blue) curves are obtained for $\rho_U = 10.1$. The top panel shows the functional dependence of $\bar{\phi}$ on $\hat{\rho}_o$. The long dashed (black) line is the asymptotic value $\bar{\phi} = \sqrt{6}\pi/4$ and the short dashed (black) line represents the disconnected solutions. The bottom panel shows the dependence of $\bar{E}$ on $\bar{\phi}$.

baryonic branch minimize the free energy. Nonetheless, this branch does not extend to $\bar{\phi} \to \pi$ any more: once $\hat{\rho}_o < \rho_*$, the new, unstable branch appears, along which asymptotically $\bar{\phi} \to 0$ for $\hat{\rho}_o \to 0$. [4] For large values

[4] In the bottom four panels of Fig. 6, the fifth (unstable) branch extends to meet the disconnected branch at $(\bar{E}, \bar{\phi}) = (0, 0)$, but

$\bar{\phi} > \bar{\phi}_c$ it is now the disconnected solution that dominates the dynamics. Hence there is a physically interesting phase transition between connected and disconnected solutions.

This result reproduces the behaviour expected for solutions with CVMN asymptotics discussed in [28], but only provided ρ_* is small. By looking at the top panel of Fig. 6, we see that if $\rho_* \gtrsim 0.5$, all the connected configurations yield $\bar{\phi} < \bar{\phi}_a$. This is the regime dominated by the short solutions. When $\rho_* > 0.5$, the disconnected configurations exist solely, with $\bar{\phi} > \bar{\phi}_a$. The physics of the D7 probes is trivial in this case, so we show only the small ρ_* examples.

For completeness, we reconsider the case in which $P \gg \hat{P}$ for every ρ. This has already been discussed in [28], where it is shown that connected configurations are always unstable, and the disconnected ones have always lower energy. Fig. 7 displays an example in this class. Notice that $\mathcal{Z}$ is positive definite. Taking into account the short connected solutions has the effect of restricting the physical range of $\bar{\phi}$. Yet, this does not affect the conclusion of [28], according to which in these backgrounds only the disconnected configurations are physically realised, meaning that the D7 system cannot describe chiral-symmetry breaking. We show this fact explicitly in Fig. 8, for a probe brane in the background of Fig. 7.

C. Summary.

We briefly summarise the results for all the possible backgrounds controlled by P_a, including both those discussed here and those that were already examined in [28]. We present a compendium in Fig. 9.

There are five possible subclasses of supersymmetric solutions to the wrapped-D5 system that are not fatally singular. For each class the probe-D7 branes behave differently. We list them here, following the same order as in the figure.

- In the CVMN case, for any value of $\bar{\phi}$ there exists only two embeddings. The connected ones physically represent the chiral-symmetry broken phase. They are classically stable (yield the correct concavity in the $(\bar{\phi}, \bar{E})$ plane, and have a negative-definite $\mathcal{Z}$), and are always the minimum of the energy. The second configuration allowed is the disconnected one, which is always disfavoured.

- A third branch appears in backgrounds distinguished by the walking scale ρ_* in the IR, but with the same UV behaviour as CVMN. This branch is classically unstable and a maximum of $\bar{E}$. It is characterised by an endpoint $\hat{\rho}_o < \rho_*$. Connected configurations with $\hat{\rho}_o > \rho_*$ are homologous to the ones of the CVMN case, but exist only for a range of $\bar{\phi} < \bar{\phi}_1$. A first-order phase transition emerges with a critical value of $\bar{\phi}_c$ that depends on ρ_*. For $\bar{\phi} > \bar{\phi}_c$ the disconnected configuration is dynamically preferred, and chiral symmetry is restored. For $\bar{\phi} < \bar{\phi}_c$ the connected solution is realised, and the model describes chiral-symmetry breaking.

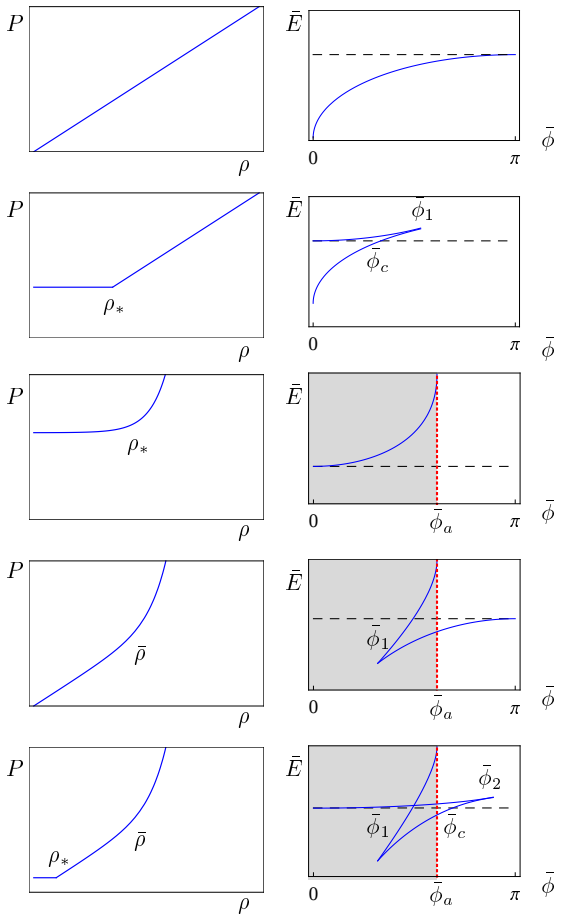

FIG. 9: Cartoons representing all the possible solutions of the form P_a to the non-Abelian wrapped-D5 system. The left panels show P as a function of ρ, while the right panels display, for the corresponding backgrounds, the connected (continuous blue lines) configurations for the probe-D7, the disconnected (long-dashed black lines), and the short connected configurations (short-dashed red lines). The actual plots, rather than these cartoons, can be found either in earlier sections or in [28]. The physical configurations are those with lowest $\bar{E}$. The shaded region to the left of the short configurations is disconnected from the continuum limit, in the sense that the results do not have an interpretation in the dual field theory.

this feature is not shown due to limitations of the numerics.

- Backgrounds described by the walking scale ρ_* in the IR, but for which P grows exponentially in the UV. There are three branches of solutions. The long connected ones exist only for $\bar{\phi} < \bar{\phi}_a = \sqrt{6}\pi/4$, are classically unstable and never a minimum of $\bar{E}$. The short connected ones, localised near the cutoff, exist for every $\bar{\phi} < \bar{\phi}_a$, are classically stable, and have divergent (negative) energy. When they exist, they dominate the dynamics. There is a bulk (first-order) phase transition at $\bar{\phi}_a$, above which the disconnected configurations yield a description of the field theory in the chiral-symmetry restored phase. Below, the gravity system is not related to the field theory.

- Backgrounds in which P is approximately linear for $\rho < \bar{\rho}$, and exponentially growing for $\rho > \bar{\rho}$. There are four branches of solutions. Two of them are long and connected, and represent a stable branch, which minimizes the energy for $\bar{\phi} > \bar{\phi}_a$, and an unstable branch that is always subdominant. These two branches exist only for $\bar{\phi} > \bar{\phi}_1$, with $\bar{\phi}_1$ a function of $\bar{\rho}$, such that $\bar{\phi}_1 < \bar{\phi}_a$. Disconnected solutions are never dominant. The short connected ones govern the dynamics for $\bar{\phi} < \bar{\phi}_a$, and a bulk phase transition takes place at $\bar{\phi}_a$. In this instance, the chiral-symmetry broken phase is the physical one connected to the field theory.

- Backgrounds represented by three scales, such that P is approximately constant in the walking region $\rho < \rho_*$, approximately linear for $\rho_* < \rho < \bar{\rho}$, and exponentially growing for $\rho > \bar{\rho}$. There are five branches of solutions. There is a first-order bulk phase transition at $\bar{\phi}_a$. Below this value the physics is not related to the field theory. Provided the scale $\rho_* \lesssim 0.5$, the physical region $\bar{\phi} > \bar{\phi}_a$ shows another first-order phase transition at $\bar{\phi}_c > \bar{\phi}_a$, such that for $\bar{\phi}_a < \bar{\phi} < \bar{\phi}_c$ the theory is in the chiral-symmetry broken phase, and for $\bar{\phi}_c < \bar{\phi} < \pi$ the symmetry is restored. For larger values of ρ_* the physical phase transition disappears, and for any $\bar{\phi} > \bar{\phi}_a$ chiral symmetry is restored. There are two turning points at $\bar{\phi}_1$ and $\bar{\phi}_2$, joining different branches, but both appear in regions that are energetically disfavoured.

We now discuss the implications for physics, in light of the idea that this scenario may be used to build models of dynamical EWSB. Given that chiral symmetry is identified with the electroweak gauge group, it is desirable that the gravity system is in the symmetry-broken phase.

This leaves us with two possibilities. The first is a background with CVMN UV-asymptotics. In this case, ρ_* is unrestricted, but the chiral-symmetry broken phase is realised only provided $\hat{\rho}_o \gtrsim \rho_*$. It would be interesting to know whether it is feasible to compute the S-parameter and construct a realistic model. For this type of backgrounds, the calculation of two-point functions are rendered difficult by the non-local behavior of their divergences in the UV. It is hence not clear at the moment how to define holographic renormalisation. On the other hand, it is known that for large values of ρ_* the spectrum of fluctuations (glueballs) contains an anomalously light scalar state. This mode is probably a dilaton and might coincide with the Higgs particle recently discovered. This is a compelling scenario that merits further inspection.

The second possibility is an exponential growth for P in the UV. Necessarily, the model contains two additional scales: $\bar{\rho}$, below which the baryonic VEV becomes important, and a rather small walking scale ρ_*, below which a dimension-six VEV manifests. The shortness of the walking region allowed by chiral symmetry breaking means that the effects of walking are probably negligibly small.

VI. CONCLUSIONS AND FURTHER DIRECTIONS.

When performing gravity calculations for the study of strongly-coupled field theories, a regulation procedure is needed. We showed that there are cases in which this may end up revealing that some regions of parameter space are not connected with the field theory. This is analog to bulk transitions in lattice gauge theories. The results obtained by naively using the regulation procedure are unaffected, as long as the calculations are performed on the right side of the bulk transition. All the answers on the wrong side of the transition must be discarded, since they are unrelated to the dual field theory. We exhibited a few examples and explained them in details. This is a further element in support of the conjectured gauge/gravity dualities.

It would be useful to find a complete (top-down) gravity system that reproduces the phenomenology of dynamical EWSB, including the fact that a Higgs particle has been observed. A particularly nice environment is that of the wrapped-D5 system in Type IIB supergravity, wherein a lot of progress has been made. Chiral symmetry breaking can be modelled by probing these geometries with D7-branes in a certain special configuration. We completed the analysis of all the possible backgrounds of this type. The results are compatible with chiral symmetry breaking only in a special subclass, for which precision parameters have not been calculated so far.

This whole program should be repeated in other families of backgrounds, starting from the more general class within the Papadopoulos–Tseytlin ansatz [40]. Some of the observations we made in this paper might provide guidance in this direction. It has been found in [17] that in the Klebanov–Strassler system there exists (mildly singular) geometries that admit a parametrically light scalar in the spectrum. It would be interesting to know whether those backgrounds could be used to model dynamical EWSB. The milder UV behaviour of these KS-like solu-

tions suggests that it might be possible to calculate the S-parameter, overcoming the difficulties one faces with the wrapped-D5 examples.

A completely new feature emerged in the scale-invariant flavoured Abelian backgrounds: the bulk transition is second-order. In the proximity of the critical point, gravity effectively describes some (unknown) CFT. It is plausible that similar situations may arise in other instances. This is potentially a novel framework to discuss new classes of CFT's, and the phenomenology related to the (explicit or spontaneous) breaking of their symmetries. For example, this might be an avenue to study the four-dimensional dilaton, turning the technical curiosity we uncovered into an approach of practical physics use.

Acknowledgments

We thank Prem Kumar, Biagio Lucini, Carlos Nuñez and Michael Warschawski for useful discussions. The work of A. F. was supported by MEC FPA2010-20807-C02-02, by CPAN CSD2007-00042 Consolider-Ingenio 2010 and finally by ERC Starting Grant "HoloLHC-306605". The work of M. P. is supported in part by WIMCS and by the STFC grant ST/J000043/1. D. S. is supported by the STFC Doctoral Training Grant ST/I506037/1.

[1] S. Weinberg, Phys. Rev. D **19**, 1277 (1979); L. Susskind, Phys. Rev. D **20**, 2619 (1979); S. Weinberg, Phys. Rev. D **13**, 974 (1976).

[2] R. S. Chivukula, arXiv:hep-ph/0011264; K. Lane, arXiv:hep-ph/0202255, C. T. Hill and E. H. Simmons, Phys. Rept. **381**, 235 (2003) [Erratum-ibid. **390**, 553 (2004)] [arXiv:hep-ph/0203079]; A. Martin, arXiv:0812.1841 [hep-ph]; F. Sannino, arXiv:0911.0931 [hep-ph]; M. Piai, Adv. High Energy Phys. **2010**, 464302 (2010) [arXiv:1004.0176 [hep-ph]].

[3] B. Holdom, Phys. Lett. B **150**, 301 (1985); K. Yamawaki *et al.* Phys. Rev. Lett. **56**, 1335 (1986); T. W. Appelquist *et al.* Phys. Rev. Lett. **57**, 957 (1986).

[4] J. M. Maldacena, Adv. Theor. Math. Phys. **2**, 231 (1998) [Int. J. Theor. Phys. **38**, 1113 (1999)] [arXiv:hep-th/9711200]; S. S. Gubser, I. R. Klebanov and A. M. Polyakov, Phys. Lett. B **428**, 105 (1998) [arXiv:hep-th/9802109]; E. Witten, Adv. Theor. Math. Phys. **2**, 253 (1998) [arXiv:hep-th/9802150].

[5] O. Aharony, S. S. Gubser, J. M. Maldacena, H. Ooguri and Y. Oz, Phys. Rept. **323**, 183 (2000) [arXiv:hep-th/9905111].

[6] S. -J. Rey and J. -T. Yee, Eur. Phys. J. C **22**, 379 (2001) [hep-th/9803001]; J. M. Maldacena, Phys. Rev. Lett. **80**, 4859 (1998) [hep-th/9803002].

[7] E. Witten, Adv. Theor. Math. Phys. **2**, 505 (1998) [arXiv:hep-th/9803131],

[8] A. Karch and E. Katz, JHEP **0206**, 043 (2002) [hep-th/0205236].

[9] K. Skenderis, Class. Quant. Grav. **19**, 5849 (2002) [arXiv:hep-th/0209067]; I. Papadimitriou and K. Skenderis, arXiv:hep-th/0404176.

[10] B. Lucini, A. Patella, A. Rago and E. Rinaldi, JHEP **1311**, 106 (2013) [arXiv:1309.1614 [hep-lat]].

[11] P. Candelas, X. C. de la Ossa, Nucl. Phys. **B342**, 246-268 (1990).

[12] J. M. Maldacena and C. Nunez, Phys. Rev. Lett. **86**, 588 (2001). [arXiv:hep-th/0008001].

[13] A. H. Chamseddine and M. S. Volkov, Phys. Rev. Lett. **79**, 3343 (1997) [arXiv:hep-th/9707176].

[14] C. Nunez, I. Papadimitriou and M. Piai, Int. J. Mod. Phys. A **25** (2010) 2837 [arXiv:0812.3655 [hep-th]].

[15] D. Elander, C. Nunez and M. Piai, Phys. Lett. B **686**, 64 (2010) [arXiv:0908.2808 [hep-th]].

[16] D. Elander and M. Piai, Nucl. Phys. B **871**, 164 (2013) [arXiv:1212.2600 [hep-th]].

[17] D. Elander, arXiv:1401.3412 [hep-th].

[18] L. Anguelova, Nucl. Phys. B **843**, 429 (2011) [arXiv:1006.3570 [hep-th]];

[19] L. Anguelova, P. Suranyi and L. C. R. Wijewardhana, Nucl. Phys. B **852**, 39 (2011) [arXiv:1105.4185 [hep-th]];

[20] L. Anguelova, P. Suranyi and L. C. R. Wijewardhana, Nucl. Phys. B **862**, 671 (2012) [arXiv:1203.1968 [hep-th]].

[21] T. E. Clark, S. T. Love and T. ter Veldhuis, Nucl. Phys. B **872**, 1 (2013) [arXiv:1208.0817 [hep-th]].

[22] L. Anguelova, P. Suranyi and L. C. R. Wijewardhana, arXiv:1306.1981 [hep-th].

[23] L. Anguelova, P. Suranyi and L. C. R. Wijewardhana, arXiv:1309.6678 [hep-th].

[24] T. Sakai and S. Sugimoto, Prog. Theor. Phys. **113**, 843 (2005) [arXiv:hep-th/0412141].

[25] S. Kuperstein and J. Sonnenschein, JHEP **0809**, 012 (2008) [arXiv:0807.2897 [hep-th]].

[26] A. Dymarsky, S. Kuperstein and J. Sonnenschein, JHEP **0908**, 005 (2009) [arXiv:0904.0988 [hep-th]].

[27] C. D. Carone, J. Erlich and M. Sher, Phys. Rev. D **76**, 015015 (2007) [arXiv:0704.3084 [hep-th]]; T. Hirayama and K. Yoshioka, JHEP **0710**, 002 (2007) [arXiv:0705.3533 [hep-ph]]. O. Mintakevich and J. Sonnenschein, JHEP **0907**, 032 (2009) [arXiv:0905.3284 [hep-th]].

[28] A. F. Faedo, M. Piai and D. Schofield, arXiv:1312.2793 [hep-th].

[29] A. Brandhuber and K. Sfetsos, Adv. Theor. Math. Phys. **3**, 851 (1999) [hep-th/9906201].

[30] S. D. Avramis, K. Sfetsos and K. Siampos, Nucl. Phys. B **769** (2007) 44 [hep-th/0612139].

[31] D. J. Gross and H. Ooguri, Phys. Rev. D **58**, 106002 (1998) [hep-th/9805129].

[32] D. Bak, A. Karch and L. G. Yaffe, JHEP **0708**, 049 (2007) [arXiv:0705.0994 [hep-th]].

[33] C. Nunez, M. Piai and A. Rago, Phys. Rev. D **81**, 086001 (2010) [arXiv:0909.0748 [hep-th]].

[34] A. Armoni, M. Piai and A. Teimouri, Phys. Rev. D **88**, 066008 (2013) [arXiv:1307.7773 [hep-th]].

[35] R. Casero *et al.* Phys. Rev. D **73**, 086005 (2006); [arXiv:hep-th/0602027] Phys. Rev. D **77**, 046003 (2008). [arXiv:0709.3421 [hep-th]].
[36] C. Hoyos-Badajoz *et al.* Phys. Rev. D **78**, 086005 (2008). [arXiv:0807.3039 [hep-th]].
[37] D. Elander, J. Gaillard, C. Nunez and M. Piai, JHEP **1107**, 056 (2011) [arXiv:1104.3963 [hep-th]].
[38] A. Butti, M. Grana, R. Minasian, M. Petrini and A. Zaffaroni, JHEP **0503**, 069 (2005) [arXiv:hep-th/0412187].
[39] I. R. Klebanov and M. J. Strassler, JHEP **0008**, 052 (2000) [arXiv:hep-th/0007191].
[40] G. Papadopoulos and A. A. Tseytlin, Class. Quant. Grav. **18**, 1333 (2001) [arXiv:hep-th/0012034].
[41] D. Cassani and A. F. Faedo, arXiv:1008.0883 [hep-th]; I. Bena, G. Giecold, M. Grana, N. Halmagyi and F. Orsi, arXiv:1008.0983 [hep-th].
[42] J. Maldacena and D. Martelli, JHEP **1001** (2010) 104 [arXiv:0906.0591 [hep-th]];
[43] E. Caceres, C. Nunez and L. A. Pando-Zayas, JHEP **1103**, 054 (2011) [arXiv:1101.4123 [hep-th]].
[44] J. Gaillard, D. Martelli, C. Nunez and I. Papadimitriou, Nucl. Phys. B **843**, 1 (2011) [arXiv:1004.4638 [hep-th]].